










Quantitative assessment of the use of Kazakhstan montmorillonite clays as sorbent carriers for pharmaceutical substances

D.K. Bolatkan¹ , A.Zh. Kerimkulova^{2*} , M.M. Beisebekov³ ,
K. Akatan¹ , N. Kantay¹ , E. Shaimardan³ , A. Kukhareva^{2,3} ,
A. Bukunova⁴  and S.K. Kabdrakhmanova² 

¹S.Amanzholov East Kazakhstan University, Ust-Kamenogorsk, Kazakhstan

²Satbayev University, Almaty, Kazakhstan

³Scientific Center of Composite Materials, Almaty, Kazakhstan

⁴D.Serikbayev East Kazakhstan Technical University, Ust-Kamenogorsk, Kazakhstan

*e-mail: kerimkulova07@mail.ru, s.kabdrakhmanova@gmail.com

(Received April 15, 2025; received in revised form May 27, 2025; accepted June 6, 2025)

Bentonite materials are widely utilized across various industries due to their unique physicochemical properties. This study presents a qualitative and comparative analysis of mineral substances derived from bentonite clay deposits in East Kazakhstan. The montmorillonite content in the samples ranges from 75.5% to 88%, with adsorption capacity (determined by the methylene blue method) varying between 119 and 204 mg/g. The pH of the samples lies within the range of 7 to 10. FTIR and XRF analyses confirmed the presence of major components such as silicon and aluminum oxides, while X-ray diffraction identified montmorillonite as the dominant crystalline phase. Textural characterization revealed specific surface areas of 94–104 m²/g, pore volumes of 0.03–0.05 cm³/g, and pore sizes between 0.8 and 1.04 nm. SEM analysis demonstrated a flaky, layered, and porous morphology typical of bentonite. Based on these properties, the bentonite samples exhibit strong potential for industrial use. They are applicable in oil production (as components of drilling fluids) and construction (as insulating and sealing agents). Additionally, their high sorption capacity makes them promising candidates for pharmaceutical applications, particularly as carriers in topical formulations such as ointments and pastes for wound healing and inflammatory skin conditions.

Keywords: bentonite clays, montmorillonite, mineral composition, surface area, physico-chemical properties.

PACS number(s): 82.70.Dd; 72.80.Tm; 82.80.–d.

1 Introduction

Currently, the development of the chemical industry, environmental degradation, the depletion of natural resources, and the increase in synthetic products have posed new challenges for scientists. One of the key objectives is to develop products derived from economically viable and accessible raw materials that do not have adverse effects on human health [1]. In this context, the study of the properties of natural clays, which belong to the category of mineral raw materials, and the identification of their potential applications in industry and everyday life, is of particular relevance.

Bentonites are natural mineral clays composed mainly of various metal oxides. Due to their chemical composition, they are widely used in the production of construction materials [2], porcelain [3], as additives in animal feed [4], and in such fields as medicine, pharmaceuticals [5], and cosmetology [6], which contributes to the growing demand for these materials.

Approximately 30% of the global bentonite reserves are located in China, 15% in the United States, and 7% in Turkey [7]. Other countries with significant bentonite resources include Greece, Russia, France, India, Turkey, Azerbaijan, Georgia, and Armenia. In Kazakhstan, large bentonite reserves are

concentrated in the southern and eastern regions [8]. In South Kazakhstan, the Dzherzhinskoye, Ildersay, and Andreevskoye deposits are estimated to contain around 100 million tons of bentonite, while the Darbaza and Keles deposits hold approximately 58 million tons [9]. In Eastern Kazakhstan, the group of deposits known as the Manyrak bentonite clays is estimated to contain up to 50 million tons [10].

The distribution of bentonites across different geographical regions, along with factors such as climate, geological structure, and local environmental conditions, contributes to the variation in their physico-chemical properties [11]. Since the formation of mineral clays is a prolonged and complex process, significant differences can also be observed in the properties of bentonites extracted from different depths within a single deposit [12]. These differences, in turn, are key factors determining the quality and potential applications of bentonitic clay. Therefore, identifying the chemical composition, phase structure, and qualitative characteristics of natural clays is of critical importance.

During geological exploration activities conducted in the 1960s, mineral clays from the Tagan deposit in Eastern Kazakhstan began to be extensively studied [9]. According to X-ray phase analysis, the bentonites of the Tagan deposit are predominantly composed of montmorillonite minerals, with quartz, feldspar, and calcite as secondary components [13].

In recent years, due to the rapid growth in oil and gas production, special attention in the exploration sector has been given to high-quality drilling fluids based on bentonite powders, which are used for well cementing. These materials are particularly relevant for exploratory offshore oil drilling. Chemically unmodified bentonite powders must possess high viscosity and relatively high static shear stress. Such properties are characteristic of the bentonites from the 14th horizon of the Tagan deposit. Furthermore, these bentonites are also used in the production of cracking catalysts for crude oil processing. The bentonite from the 12th horizon of the Tagan deposit is notable for its high content of montmorillonite in alkaline form, which serves as the base material for the pharmaceutical product Tagansorbent. This drug is designed for the removal of heavy metal ions and is used in cases of poisoning, diarrhea, and intoxication [14].

In the 1990s, the physico-chemical properties of bentonites from the Tagan deposit were studied, leading to an expansion in their fields of application [14]. According to studies [14, 15], the montmorillonite content in Tagan deposit bentonites was reported to

be 90–92%, which directly contributes to their high binding capacity, as well as their adsorption and catalytic activity [16].

The potential use of sulfuric acid-modified bentonite from the 14th horizon of the Tagan deposit for the removal of Cu^{2+} , Pb^{2+} , Cd^{2+} , and Zn^{2+} heavy metal ions from mining wastewater has been investigated in studies [17, 18]. These studies revealed that the degree of sorption of heavy metal ions reached 90–98%. Furthermore, in the study [19], to increase the surface area and enhance the sorption capacity of Tagan bentonites, thermal activation at 120 °C for 4 hours followed by treatment with sulfuric acid for 2 hours increased the specific surface area up to 85 m²/g.

In addition, the abundance of micro- and macroelements in Tagan bentonites has enabled the use of clay from the 12th horizon for pharmaceutical purposes [20]. At present, bentonite is used as an enterosorbent in the form of a ready-made product to remove accumulated toxins and radionuclides from the human body. It can also be applied as an antacid to neutralize excess stomach acid [21]. Furthermore, studies [22, 23] have shown the high potential for using this clay horizon as a feed additive.

In conclusion, based on the results of the conducted literature review, it has been determined that further research aimed at expanding the application areas of bentonite clay remains highly relevant due to its unique properties. Accordingly, this study presents a comparative analysis of the physico-chemical properties of bentonites distributed in the East Kazakhstan region, with a particular focus on their potential application in medicine.

2 Experimental section

2.1 Materials

Chrysoidin 6 W, Rhodamine ($\text{C}_{21}\text{H}_{16}\text{N}_2\text{O}_3 \cdot \text{HCl}$ $\geq 85\%$ (HPLC)), Trilon B, Methylene blue, sodium pyrophosphate, ethanol (96%, $\text{C}_2\text{H}_5\text{OH}$), sulfuric acid (98%, H_2SO_4), sodium hydroxide ($\geq 99\%$, NaOH), potassium bichromate ($\geq 99\%$, $\text{K}_2\text{Cr}_2\text{O}_7$), sodium thiosulfate (99%, $\text{Na}_2\text{S}_2\text{O}_3$), potassium iodide ($\geq 99\%$, KI) obtained from Sigma-Aldrich (Bangalore, India). All other reagents were of analytical grade a- were used without additional purification.

2.2 Methods

2.2.1 Raw materials

Three different bentonite samples were collected for the study from clay deposits in the East Kazakhstan region, which are known to contain re-

serves of alkali and alkaline earth metal bentonites. Sampling of bentonite clay was carried out at three discrete and representative points of the Tagan deposit at a depth of 1.5 meters, selected in advance based on geological exploration data and clay stratum mapping. To ensure the reliability of the analysis and reflect the spatial heterogeneity of the raw material, each sample was manually extracted using the trenching method. The sampling sites were located within a single clay bed, evenly distributed to avoid areas of intensive weathering or anthropogenic impact. The collected samples, each with a volume of 50 mL and a diameter of 10 mm, were ground using a FRITSCH-6 (GERMANY) planetary ball mill at a temperature of 25 ± 2 °C, with a rotation speed of 300 rpm for 15 minutes. The ground material was then sieved through a 0.01 mm mesh. The bentonite samples used in the study were conditionally labeled as B₁, B₂, and B₃.

2.2.2 *Quality indicators bentonites*

The moisture content of the bentonite samples was determined in accordance with ASTM D2216 “Standard Test Methods for Laboratory Determination of Water (Moisture) Content of Soil and Rock by Mass”. The ash content was measured following ASTM D2974 “Standard Test Methods for Determining the Water (Moisture) Content, Ash Content, and Organic Material of Peat and Other Organic Soils”. The mass fraction of montmorillonite in the bentonite was determined according to GOST 28177-89.

The sorption capacity based on methylene blue and the pH level were determined in accordance with pharmacopoeial standard [18]. The adsorption capacity of bentonite clays was determined in accordance with the methodology outlined in the State Pharmacopoeia of the Russian Federation, based on the sorption of methylene blue from aqueous solution. A pre-weighed amount of air-dried clay sample was mixed with a methylene blue solution of known concentration and allowed to interact under controlled conditions. The mixture was stirred and maintained at room temperature for a contact time of 60 minutes. After equilibration, the suspension was filtered, and the residual concentration of methylene blue was measured spectrophotometrically at 667 nm. The adsorption capacity was calculated from the difference between the initial and final dye concentrations, expressed in mg/g of dry sorbent. Experimental parameters such as contact time, pH (maintained near neutral), and solution concentration were standardized in accordance with pharmacopoeial guidelines to ensure reproducibility and accuracy.

2.2.3 *XRF analysis*

To determine the main oxide composition of the bentonite clay, energy-dispersive X-ray fluorescence spectroscopy (EDXRF) was employed. The analysis was performed using the NEX CG II instrument (Rigaku, Japan). This device is based on a fully dispersive optical system and features a highly sensitive detector utilizing anisotropic X-ray radiation.

2.2.4 *X-ray diffraction analysis*

The structural and phase composition of the samples was investigated using X-ray diffraction (XRD) on an X'Pert PRO diffractometer (Malvern Panalytical Empyrean, Netherlands) with monochromatized copper radiation ($\text{CuK}\alpha$, K-Alpha1 [\AA] = 0.1542) and a scanning step of 0.02° . During the analysis, the measurement angle ranged from 10° to 80° , with an X-ray tube voltage of 45 kV and a current of 30 mA. The measurement time per step was 0.5 seconds, and a universal aluminum sample holder (PW1172/01) was used. The obtained XRD patterns were analyzed using the ICDD PDF-4/AXIOM XRD database.

The formula for calculating the interplanar spacing d in X-ray diffraction analysis is based on Bragg's Law:

$$2d\sin \theta = n\lambda \rightarrow d = \lambda / (2\sin \theta) \quad (1)$$

2.2.5 *FTIR analysis*

The chemical structure of the bentonite samples was analyzed using FTIR (FT-801 IR Spectrometer, Simex, Russia) in the wavelength range of 500–4000 cm^{-1} with a resolution of 1 cm^{-1} at a temperature of 25 ± 2 °C and 100 scans. During the analysis, the clay powder was mixed with potassium bromide in a 1:9 ratio and ground in an agate mortar until a fully homogeneous mixture was achieved. Subsequently, a tablet was prepared using a press in a die at 200 MPa pressure, and water vapor was drawn using a vacuum pump for 5 minutes to form the tablet.

2.2.6 *SEM analysis*

The surface morphology of the mineral clays was investigated using a 3D-SEM instrument, Quanta 200 (FEI, Netherlands). Measurements were conducted in high vacuum mode using a secondary electron detector with an accelerating voltage of 5 kV. The surface of the mineral clays was coated with gold nanoparticles to enhance electron transfer.

2.2.7 *BET analysis*

The specific surface area and pore characteristics of the clay were investigated using the BSD-660S A3

Physical Adsorption Analyzer based on low-temperature adsorption of liquid nitrogen. The analysis was conducted at a temperature of 30°C for a duration of 120 minutes. The specific surface area of the samples was determined using the BET method, while the pore characteristics were analyzed using the BJH (Barrett-Joyner-Halenda) method.

2.2.8 Thermogravimetric analysis

The thermal characteristics were studied with a LabSysevo differential thermogravimetric analyzer (Setaram, France), in an argon atmosphere. The temperature range was 30±5 – 700±5°C, with a heating rate of 10±1°C/min. The mass of the samples was approximately 25±2 mg.

2.2.9 Average particle size and Zeta potential

The zeta potential was measured using a Malvern Zetasizer Nano ZS90 instrument (UK). The Zetasizer systems utilize electrophoretic light scattering (ELS) and dynamic light scattering (DLS) methods, which provide information on the mobility, charge, and size of particles in dispersive systems ranging from nanometers to micrometers. For each sample, 12 scans were performed per run, with a total of 3 runs conducted. The entire experiment was repeated at least three times. The particle charge (zeta potential) was determined by

performing 12 scans, with a minimum of 3 runs recorded. Error bars were obtained using the standard zeta potential software.

3 Results and discussion

3.1 Preparation of raw materials

The colors of mineral clays vary widely depending on the types and quantities of chemical elements they contain [24]. The colors of the samples selected for the study ranged from light to dark brown, as shown in Figure 1.

The B₁ bentonite (Figure 1a) has a light color. The light color of the B₁ sample likely results from its montmorillonite content and its classification as an alkaline and alkaline earth type bentonite, as identified in the study [25]. Clays of this type are known to exhibit high adsorptive properties, swelling in water, and high plasticity [26].

On the other hand, the B₂ and B₃ samples are brownish-red in color (Figure 1b, 1c). This indicates the presence of iron oxides and other metal oxides in the clay composition [6]. Such mineral clays are known to be thermally stable, possess high strength, and exhibit good adsorptive properties [27]. According to [28], colored bentonite clays can be used for the production of ceramic glazes, porcelain dishes, and construction materials.



Figure 1 – Bentonite samples: a – B₁; b – B₂; c – B₃.

3.2 Quality indicators of bentonites

The results of the qualitative analysis of the bentonite clays are shown in Table 1. Determining the qualitative composition of bentonites allows for a better understanding of their potential applications. The quality of bentonite clays depends on the content and ionic form of montmorillonite [29]. In the B₁ bentonite, the mass fraction of montmorillonite was 88%, with a pH value of 8.9. In B₂ bentonite, the montmorillonite content was 75.5%, and the pH

value was 8.1, while in B₃ bentonite, the montmorillonite content was 83%, and the pH value was 7.1. According to the pharmacopeial article, the pH of bentonite clays should range from 7 to 10, and their methylene blue adsorption capacity should be no less than 150 mg per gram for their high potential in pharmaceutical applications [30]. Based on this pharmacopeial guideline, it can be concluded that the B₁ and B₂ samples have a higher potential for use in pharmaceuticals. Moreover, the closer the pH of the

bentonites is to a basic medium, the higher their ion exchange properties [31].

The methylene blue adsorption capacity reached its highest value of 204.4 mg/g in the B₁ sample. In the B₂ sample, the capacity was 119.88 mg/g, while in the B₃ sample, it was 150 mg/g.

Additionally, the moisture content of the bentonite clays ranged from 7.3% to 7.8%, which is consistent with the norm of 8% indicated in the pharmacopeial article (Table 1). This confirms the potential of the bentonite clays studied for use in pharmaceutical production.

Table 1 – Qualitative properties of bentonites.

Quality indicators			
	B ₁	B ₂	B ₃
Mass fraction of montmorillonite, %	88.0±0.02	75.5±0.21	83.0±0.5
Mass fraction of moisture, %	7.8±0.02	7.2±0.05	7.3±0.31
Mass fraction of ash content, %	14.04±0.41	15.1±0.14	14.17±0.21
Sorption capacity, mg/g	204.4±1	119.88±5	182.02±6
pH	8.9±0.5	8.1±0.3	7.1±0.4

3.3 XRF analysis

The comparative elemental composition of the bentonite clays is presented in Table 2. The main constituents of the bentonite are silicon and aluminum oxides. According to the obtained results, in sample B₁, SiO₂ was found to be 71.5%, Al₂O₃ – 21.0%, MgO – 3.67%, CaO – 1.98%, Fe₂O₃ – 1.43%, TiO₂ – 0.135%, K₂O – 0.0240%, and As₂O₃ – 0.0004%. In sample B₂, the composition was SiO₂ – 70.1%, Al₂O₃ – 17.2%, Fe₂O₃ – 6.62%, MgO – 2.85%, CaO – 1.78%, TiO₂ – 0.799%, K₂O – 0.0220%, and As₂O₃ – 0.0010%. In sample B₃, the composition was SiO₂ – 69.4%, Al₂O₃ – 16.7%, Fe₂O₃ – 8.58%, MgO – 2.44%, CaO – 0.965%, TiO₂ – 0.95%, K₂O – 0.0297%, and As₂O₃ – 0.013%.

From these values, it can be observed that the content of aluminum and silicon oxides is significantly higher, as these oxides are rock-forming oxides and are part of the main composition of the

bentonite crystal lattice [32], which is confirmed by the results where spectra corresponding to the bonds of these compounds were identified. Furthermore, the reddish-brown coloration in the samples B₂ and B₃ indicates an increased iron content, 6.62% and 8.58%, respectively. Bentonites B₁ has a relatively low iron oxide content (1.43%).

In addition, the concentrations of trace metal oxides were determined as follows: in sample B₁, Cr₂O₃ – 0.0021%, PbO – 0.0003%, and As₂O₃ – 0.0004%; in sample B₂, Cr₂O₃ – 0.175%, PbO – 0.0025%, and As₂O₃ – 0.0010%; in sample B₃, Cr₂O₃ – 0.0199%, PbO – 0.0035%, and As₂O₃ – 0.0013%. Among these, only sample B₁ meets the maximum permissible concentrations specified by the relevant pharmacopeial standards. Therefore, this sample can be considered safe in terms of toxic heavy metal content and is deemed suitable for medical use.

Table 2 – XRF analysis results of bentonites.

Composition	B ₁	B ₂	B ₃	Composition	B ₁	B ₂	B ₃
MgO, %	3.67	2.85	2.44	GeO ₂ , %	0.0002	-	0.0006
Al ₂ O ₃ , %	21.0	17.2	16.7	As ₂ O ₃ , %	0.0004	0.0010	0.0013
SiO ₂ , %	71.5	70.1	69.4	SeO ₂ , %	0.0002	0.0009	0.0010
P ₂ O ₅ , %	-	0.0826	0.0997	Br, %	-	0.0001	0.0002
SO ₃ , %	0.0387	0.192	0.494	Rb ₂ O, %	0.0004	0.0005	0.0004
Cl, %	0.0043	0.0046	0.0159	SrO, %	0.358	0.0380	0.0332
K ₂ O, %	0.0240	0.0220	0.0297	Y ₂ O ₃ , %	0.0008	0.0023	0.0026

Continuation of the table

Composition	B ₁	B ₂	B ₃	Composition	B ₁	B ₂	B ₃
CaO, %	1.98	1.78	0.965	Nb ₂ O ₅ , %	-	0.0028	0.0034
TiO ₂ , %	0.135	0.799	0.952	Ag ₂ O, %	0.0008	-	0.0007
V ₂ O ₅ , %	0.0037	0.0259	0.0343	SnO ₂ , %	0.0076	0.0079	0.0074
Cr ₂ O ₃ , %	0.0021	0.175	0.0199	Sb ₂ O ₃ , %	0.0010	0.0011	0.0010
MnO, %	0.105	0.129	0.148	TeO ₂ , %	0.0039	0.0036	0.0034
Fe ₂ O ₃ , %	1.43	6.62	8.58	I, %	-	-	-
Co ₂ O ₃ , %	0.0158	0.0294	0.0333	BaO, %	-	0.0572	0.0311
NiO, %	0.0162	0.0112	0.0102	HfO ₂ , %	0.0095	0.0111	0.0110
CuO, %	0.0040	0.0058	0.0056	Ta ₂ O ₅ , %	-	-	(0.0007)
ZnO, %	0.0021	0.0026	0.0028	WO ₃ , %	-	0.0020	-
PbO, %	0.0003	0.0025	0.0035	U ₃ O ₈ , %	0.0006	0.0008	0.0010
Ga ₂ O ₃ , %	0.0008	0.0038	0.0048	Ir ₂ O ₃ , %	0.0004	0.0007	-

3.4 Average particle size and zeta potencial

One of the important parameters that describe the colloidal properties of bentonite is the average particle size and zeta potential. These parameters allow for the evaluation of the stability of suspensions and the degree of particle aggregation.

The charge of the bentonite samples studied (B₁, B₂, and B₃) was found to be -13.6 mV, -16.6 mV, and -16.2 mV, respectively (Table 3). These nega-

tive values are due to uncompensated charges in the crystal lattice resulting from isomorphic substitution, where trivalent cations replace tetravalent silicon atoms in the tetrahedral structure and aluminum in the octahedral sites, leading to a negative zeta potential [33]. The negative zeta potential is significant for drug delivery systems, as it facilitates the transport of positively charged drug molecules, allowing for controlled release and sustained dosing [34, 35].

Table 3 – Average particle size and zeta potencial of bentonite clay.

Sample	B ₁	B ₂	B ₃
Size. nm	1614±50	1534±35	1409±15
Zeta potencial	-13.6±1	-16.6±2	-16.2±2

The negative charge of bentonite clays significantly expands their potential applications. The negatively charged bentonite particles repel each other due to electrostatic repulsion forces. This interaction influences the stability of colloidal suspensions and their rheological properties, preventing aggregation and sedimentation [36].

This property is crucial in fields like drilling fluid formulation, where viscosity control is essential for efficient oil well drilling and the prevention of wellbore collapse [37]. Moreover, negatively charged bentonite clays attract heavy metal ions and organic pollutants to their surface, exhibiting strong adsorptive properties. They can also interact with polyelectrolytes, forming stable complexes [38]. These interactions can enhance the mechanical

properties and adhesion of composite materials used in coatings.

Most importantly, the combination of nonionic or negatively charged polymers with positively charged pharmaceutical substances allows for the creation of various composites for the production of extended-release drug formulations [39].

3.5 FTIR analysis

The comparative FTIR spectra of the bentonite samples used in the study are shown in Figure 2. The analysis of these spectra reveals two key regions that provide information about the chemical structure and composition of the bentonite.

The analysis of the spectra demonstrates a clear visual similarity between the samples. The first re-

gion of the spectrum, in the range of 3700–3400 cm^{-1} , is associated with the valence vibrations of hydroxyl groups coordinated with cations in Al-OH [40]. These hydroxyl groups play a critical role in the interlayer interactions and determine properties of the clay, such as swelling and adsorptive characteristics [41]. In this region, all the samples exhibit a sharp absorption band at 3620–3600 cm^{-1} due to the presence of water molecules, which are associated with the clay matrix through hydrogen bonds [42]. Water absorbed in the crystalline lattice also contributes to the hydration and swelling of the clay.

Additionally, all the samples show an absorption band in the range of 1635–1615 cm^{-1} , which corresponds to asymmetric OH-stretching of water and is a structural element of the clay [43].

The second region of the spectrum, in the range of 1150–500 cm^{-1} , contains information about the silicate structure of the clays. In this region, absorption bands characteristic of the Si-O bond vibrations in the tetrahedral layers of the clay are observed [44].

The presence of these bands confirms the presence of silicate layers, which form the main structure of the clays.

In the B_1 sample, peaks are present in the areas of 1028–1008 cm^{-1} , corresponding to stretching vibrations and characteristic of layered silicate minerals. These peaks are associated with the threefold degenerate Si-O stretching vibrations [45]. All the samples exhibit a sharp peak in the region of 986–968 cm^{-1} , corresponding to OH-deformation modes of Al-Al-OH or Al-OH-Al [46]. A band observed in the B_1 sample at 902–895 cm^{-1} corresponds to the OH-deformation mode of Al-Al-OH or Al-OH-Al [37]. Additionally, the absorption band at 797 cm^{-1} in the B_2 sample is characteristic of the symmetric valence stretching vibrations of Si-O-Si in tetrahedral SiO_4 units [47].

The XRF analysis results confirm that the main composition of the bentonite clays consists of aluminosilicates (Table 2). The FTIR analysis results align with the XRF findings.

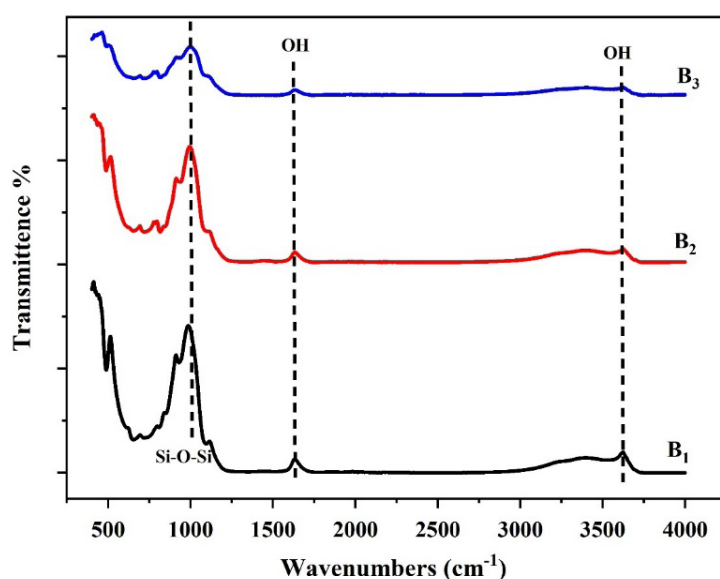


Figure 2 – FTIR Spectra of bentonite samples.

3.6 X-ray diffraction analysis

The crystallinity of mineral clays and the form of metal ions are very important indicators that determine their thermal and mechanical properties. Figure 3 shows the comparative X-ray diffractograms of the samples under investigation.

The analysis of the X-ray diffraction patterns of all the investigated samples revealed a significant similarity in the nature of the diffraction peaks. The

main diffraction reflections, presented in Table 4, are observed at 2θ angles of 19.72° (003), 25.10° (020), 35.85° (200), and 61.91° (130).

The diffractogram of sample B_1 revealed phases corresponding to the hexagonal lattice of silicon dioxide, the tetragonal modification of aluminum oxide, the cubic lattice of magnesium oxide, and a complex compound containing Al, Si, and Fe elements, which corresponds to the findings of the IR spectroscopy.

copy. These characteristics indicate that the sample belongs to the mineral phase of montmorillonite. In the B_1 sample, peaks corresponding to montmorillonite dominate, with characteristic 2θ values at 19.72° (003), 25.10° (020), 35.85° (200), and 61.91° (130). Quartz peaks, including the main peak at 26.62° (101), are weakly expressed.

In samples B_2 and B_3 , phases with a hexagonal structure of silicon dioxide, an orthorhombic modification of aluminum oxide, a hexagonal lattice of sodium oxide, and cubic-centered magnesium oxide elements were identified. Signs of monoclinic modification of montmorillonite were also observed. The intensity of the peak corresponding to quartz is more pronounced at 2θ 26.62° (101), where the interplanar distance is 3.35 \AA .

Montmorillonite demonstrates a broad, diffuse, and asymmetric basal reflection, indicating high dispersion and low crystallinity of this mineral. The main minerals in the composition of bentonite are montmorillonite (M) and quartz (Q). This corresponds to the findings that the main composition of the bentonite samples, as shown in Table 1, consists of montmorillonite.

X-ray diffraction analysis of the bentonite clay samples revealed interplanar spacings characteristic of their mineralogical composition. Reflections observed at $d = 4.91 \text{ \AA}$ and $d = 2.50 \text{ \AA}$ correspond to the (003)/(020) and (130) planes of montmorillonite, respectively. These peaks are indicative of a well-

ordered layered structure and confirm the presence of crystalline montmorillonite in the samples. In particular, the (130) reflection at 2.50 \AA is often used as a diagnostic feature of crystallinity and may reflect the distribution of cations within the octahedral sheets. The interlayer spaces oriented perpendicular to these planes typically host exchangeable cations such as Na^+ and Ca^{2+} , which are electrostatically bound and contribute significantly to the clay's sorptive and ion-exchange properties. Additionally, diffraction peaks at $d = 4.28 \text{ \AA}$ and 3.35 \AA correspond to quartz, indicating the presence of crystalline silica as an accessory phase. The presence of quartz may reduce the overall sorption capacity of the clay by diluting the montmorillonite content and decreasing the specific surface area available for adsorption.

Table 4 – Values of d-spacing, diffraction angles (2θ), and hkl.

Mineral	$2\theta(^{\circ})$	d-spacing (\AA)	hkl
Montmorillonite	19.72	4.91	003
	25.10	4.50	020
	35.85	2.55	200
	61.91	2.50	130
Quartz	20.73	4.28	100
	26.62	3.35	101
	39.39	2.29	102
	42.49	2.12	200
	50.14	1.82	112

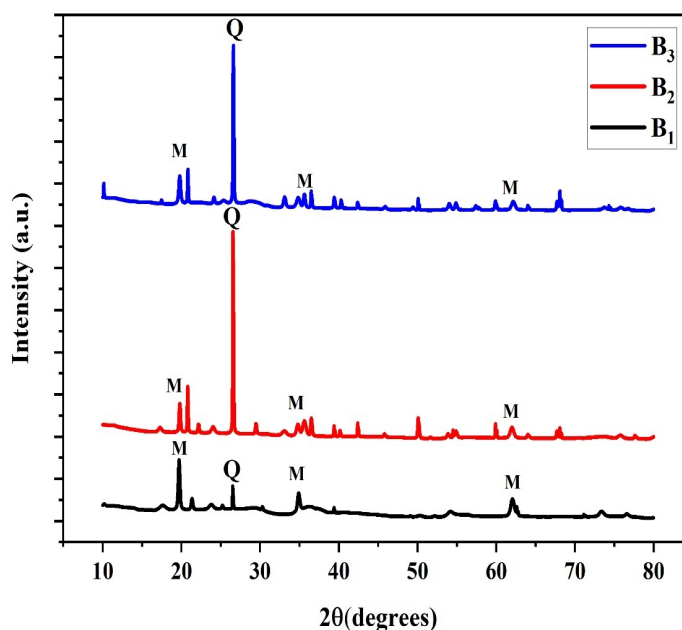


Figure 3 – B_1 ; B_2 ; B_3 XRD Spectra of bentonites.

3.7 SEM analysis

The morphological characteristics of the bentonites studied are shown in Figure 4. The results indicate that the shapes and sizes of the bentonite samples vary. Bentonitic particles are found in rhombohedral, elliptical, and square shapes. The particle sizes range from approximately 170 nm to 70 μm .

Sample B₁ has a scaly structure with an irregular shape. Additionally, the smaller particles have undergone agglomeration, and the size of the agglomerates ranges from 11.53 μm to 34 μm .

Sample B₂ consists of lamellar, plate-like, scaly particles that have formed larger particles due to agglomeration. Their sizes vary up to 203.2 nm. The B₂

sample, compared to the others, shows a plate-like, flaky, and porous structure. The flaky-porous structure is often typical for montmorillonite clays, as identified in previous studies [47].

Sample B₃ consists of solid particles with a rough surface, and their sizes range from 170.1 nm to 297.6 nm. This structure indicates a large surface area of the material, which, in turn, contributes to the high adsorption properties of the bentonites [12].

The high adsorption values of the bentonites for methylene blue, as shown in Table 1, correspond to their surface structure, as identified in the SEM analysis. This suggests that the bentonites studied have high potential for use as adsorbents.

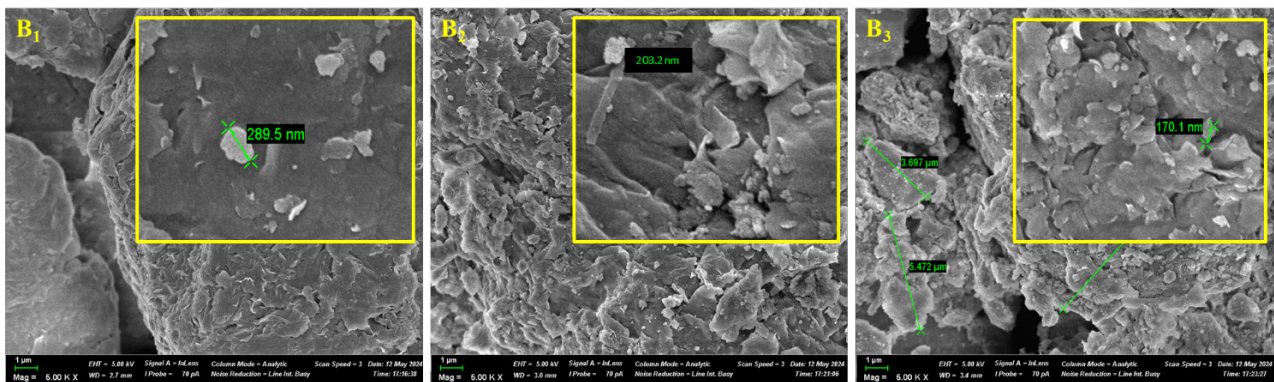


Figure 4 – The morphology of B₁, B₂ and B₃ bentonites.

3.8 BET analysis

The BET method was used to determine the specific surface area, average pore size, and volume of the bentonite samples. The specific surface area determined by the BET method describes the adsorptive capacity of the samples. On the other hand, pore volume and size reflect the diversity of their internal structure. The nitrogen adsorption-desorption isotherms of all the samples are shown in Figure 5 and Table 5.

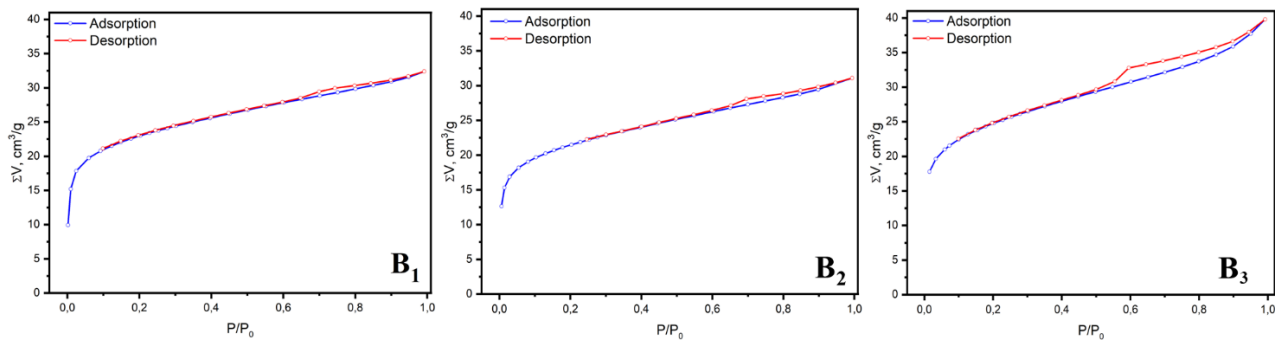
The specific surface area and pore volume and size of bentonites are among the most important parameters that characterize their adsorptive properties. Based on the research results, it was observed that the isotherms of all the samples correspond to type 4 in the Brunauer classification and exhibit hysteresis loops typical of type 2. This indicates that the sorption process starts in mesopores and ends in micropores [43].

According to the obtained results, the specific surface area of the bentonite clays, depending on

their adsorptive properties, was as follows: for sample B₁, 104.39 m²/g; for B₂, 96.55 m²/g; and for B₃, 102.87 m²/g. For B₁, the pore volume and size were 0.05 cm³/g and 0.65 nm, indicating that it is microporous. This also correlates with the highest adsorption capacity for methylene blue, which was found to be 204.4 mg/g for B₁ bentonite (Table 1) [48]. The pore volume of sample B₂ was 0.03 cm³/g with an average pore size of 0.83 nm, while for B₃, these values were 0.04 cm³/g and 1.04 nm, respectively, indicating a higher proportion of mesopores. Based on the specific surface area and pore volume, the optimal parameters were found to belong to sample B₁. According to a study [49], the surface area of the bentonites analyzed ranged from 103 to 130 m²/g, making them highly suitable for use as adsorbents. Consequently, it can be seen that the B₁, B₂, and B₃ samples from this study also have great potential for use in the preparation of biomedical products.

Table 5 – BET Analysis of bentonites.

	B₁	B₂	B₃
S (mL/g)	104.39±5	96.55±3	102.87±5
Pore volume (cm³/g)	0.05±5	0.03±4	0.04±3
Pore size (nm)	0.83±6	0.83±4	1.04±3

**Figure 5** – Adsorption-desorption isotherms of bentonites.

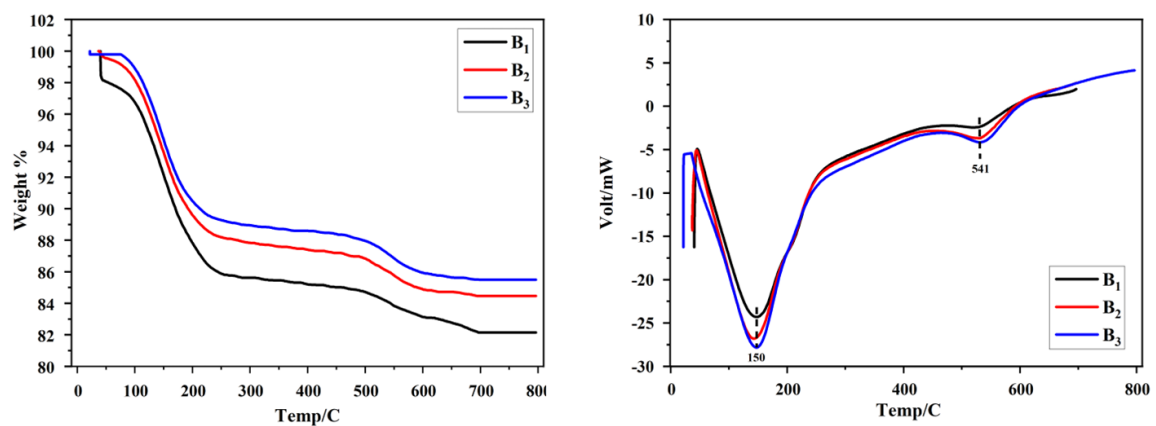
3.9 Thermogravimetric analysis

The relative TGA (Thermogravimetric Analysis) and DTA (Differential Thermal Analysis) thermograms of the bentonites are shown in Figure 6. The thermodegradation of all samples can be divided into three stages. The B₁ sample differs from the other samples in that it loses 3% of its mass at 360°C, which confirms the higher moisture content of the B₁ bentonite, as indicated in Table 1. Additionally, compared to the other two samples, B₁ loses more mass in each stage. When the temperature rises to 240°C, the weight of B₁ and B₂ samples decreases by 11%, while the B₃ sample decreases by 10%. This change cor-

responds to the amount of absorbed moisture on the bentonite surface and in the interlayer spaces [50].

The second change occurs in the temperature range of 250°C-500°C, where the mass of all samples decreases by approximately 2.5%. This may be related to the dehydration of crystallized water that is tightly bound to the montmorillonite mineral in the bentonite [51].

The third change occurs in the temperature range of 500°C-700°C, when the crystalline structure of the mineral in the bentonite begins to undergo destruction. This is accompanied by structural changes and the loss of the original mineralogical structure.

**Figure 6** – The TGA-DTA graphs of bentonites.

The analysis of the DTA curves for all three samples (B_1 , B_2 , B_3) revealed two distinct endothermic effects. The first, intense endothermic peak is observed around 150°C, and is likely associated with the removal of physically adsorbed and interlayer water. This thermal effect is recorded in all samples with slight variations in intensity. The most pronounced effect is observed in the B_1 sample, which may indicate an increased moisture content in the structure of this sample.

The second endothermic peak is recorded around 541°C and is interpreted as the result of dehydration, accompanied by the destruction of the crystalline structure of montmorillonite and the removal of structurally bound hydroxyl groups.

4 Conclusion

The results of the conducted research showed that the physicochemical properties of the obtained bentonite samples were thoroughly studied. The mineralogical composition, determined using X-ray phase analysis and IR spectroscopy methods, revealed that the main mineral component of all samples is aluminosilicates. Additionally, it was shown that the primary mineral constituting bentonite corresponds to montmorillonite. The elemental composition, analyzed using the XRF method, confirmed the presence of elements characteristic of the montmorillon-

ite mineral in the bentonite, including SiO_2 , Al_2O_3 , Fe_2O_3 , MgO , and CaO . According to the obtained results, the montmorillonite content was 88% in the B_1 sample, 75.5% in the B_2 sample, and 83% in the B_3 sample. The methylene blue adsorption capacities were 204.4 mg/g for B_1 , 119.88 mg/g for B_2 , and 182.02 mg/g for B_3 . The pH values of the medium were 8.9 for B_1 , 8.1 for B_2 , and 7.1 for B_3 .

In terms of texture parameters, the specific surface area for the B_1 sample was 104.39 m²/g, the pore volume and size were 0.05 cm³/g and 0.83 nm, respectively, and the zeta potential was -13.6. For the B_2 sample, the surface area was 96.55 m²/g, the pore volume and size were 0.03 cm³/g and 0.83 nm, respectively, and the zeta potential was -16.6. For the B_3 sample, the surface area was 102.87 m²/g, the pore volume and size were 0.04 cm³/g and 1.04 nm, respectively, and the zeta potential was -16.2.

The results demonstrate that bentonite clays possess strong potential for use as adsorbents and as drug carriers in biomedical applications. Additionally, further research is needed to explore their application as a main component in composite materials.

Acknowledgments This work was supported by the Science Committee of the Ministry of Science and Higher Education of the Republic of Kazakhstan, Grant No. AP19680576.

References

1. Bangar, S. P., Ilyas R., Chowdhury A., Navaf M., Sunooj K. V., Siroha A. K. Bentonite clay as a nanofiller for food packaging applications // *Trends in Food Science & Technology*. – 2023. – Vol. 142. – Is. 15. – P.104-242. <https://doi.org/10.1016/j.tifs.2023.104242>
2. Thakkar K., Sre M., Ballari S. O., Yadav M. K. D., Bansode M. S. S., Shukla M. S. Application of bentonite clay as a binding material // *Design Engineering*. – 2021. – Vol. 3. – Is. 9. – P. 9111-9131.
3. Boussac H., Chemani H., Serier A. Characterization of porcelain tableware formulation containing bentonite clay // *International Journal of Physical Sciences*. – 2015. – Vol. 10. – Is. 1. – P. 38-45. <https://doi.org/10.5897/IJPS2014.4218>
4. Rychen G., et. al. Safety and efficacy of bentonite as a feed additive for all animal species // *EFSA Journal*. – 2017. – Vol. 15. – Is. 12. – Art. e05096. <https://doi.org/10.2903/j.efsa.2017.5096>
5. Todorovic B.Z., Stojiljković S. T., Stojiljković M. S., Pertovic S.M., Takic L.M., Stojiljković D.T. Removal of As³⁺ cations from water by activated charcoal, bentonite and zeolite in a batch system at different pH*1 // *Journal of Elementology*. – 2017. – Vol. 22. – Is. 2. – P.713-723. <https://doi.org/10.5601/jelem.2016.21.3.1247>
6. Sarruf F. D., Contreras V. J. P., Martinez R. M., Velasco M. V. R., Baby A. R. The scenario of clays and clay minerals use in cosmetics/dermocosmetics // *Cosmetics*. – 2024. – Vol. 11. – Is. 7. <https://doi.org/10.3390/cosmetics11010007>
7. Khamroyev J., Akmalaiuly K., Fayzullayev N. Mechanical activation of navbahorsk bentonite and its textural and adsorption characteristics // *News of the National Academy of Sciences of the Republic of Kazakhstan, Series of Geology and Technical Sciences*. – 2022. – Vol. 1. – Is. 451. – P.167-174. <https://doi.org/10.32014/2022.2518-170X.154>
8. Starý J., Jirasek J., Ptíčen F., Zahradník J., Sivek M. Review of production, reserves, and processing of clays (including bentonite) in the Czech Republic // *Applied Clay Science*. – 2021. – Vol. 205. <https://doi.org/10.1016/j.clay.2021.106049>
9. Belousov P., Krupskaya V. Bentonitovye gliny Rossii i stran blizhnego zarubezh'ya // *Georesursy*. – 2019. – Vol. 21. – P.79-90. (In Russian)
10. Orudzheva D.S., Obukhov A.N. Zaysan Depression. Petroleum Geology // *A Digest of Russian Literature on Petroleum Geology*. – 1991. – Vol. 25. – Is. 7/8. – P.1278-280.

11. Sapargaliyev Y., Sapargaliyeva L., Dolgoplova A., Azelkhanov A., Suyekpayev E. Applications Of montmorillonite from the Tagan Deposit, Kazakhstan // *Global Advanced Research Journal of Engineering, Technology and Innovation*. – 2015. – Vol. 4. – P. 041-050.
12. Pan T., Chen J., He M.Y., Ding C., Ma Y., Liang H., Zhang T., Du X. Characterization and resource potential of Li in the clay minerals of Mahai Salt Lake in the Qaidam Basin, China // *Sustainability*. – 2023. – Vol. 15. – Art. 14067. <https://doi.org/10.3390/su151914067>
13. Krupskaya V., Zakusin S., Tyupina E., Dorzhieva O., Chernov M., Bychkova Y.V. Transformation of the montmorillonite structure and its adsorption properties due to the thermochemical treatment // *Geochemistry*. – 2019. – Vol. 64. – P.300-319. (In Russian).
14. Sapargaliyev E.M. Genesis features of the Tagansky field of bentonites in the Zaysan depression // *Messenger of Ore Deposits*. – 2007. – Vol. 3. – P.40-46.
15. Izosimova Y., Gurova I., Tolpeshta I., Karpukhin M., Zakusin S., Zakusina O., Samburskiy A., Krupskaya V. Adsorption of Cs (I) and Sr (II) on bentonites with different compositions at different pH // *Minerals*. – 2022. – Vol. 12. – Art. 862. <https://doi.org/10.3390/min12070862>
16. Suiekpayev Y., Sapargaliyev Y., Dolgoplova A., Selmann R., Raspopov A., Bekenova G. Predictive estimate of Ti-Zr placer deposits in mesozoic and cenozoic sediments at nw margins of the Zaysan basin, East Kazakhstan // *NEWS of National Academy of Sciences of the Republic of Kazakhstan. Series of geology and technical sciences*. – 2019. – Vol. 2.-Is. 434. – P.6-14. <https://doi.org/10.32014/2019.2518-170X.32>
17. Muzdybayeva S., Musabekov K., Muzdybayev N., Askarova G., Nurbaeva N., Taybaeva P. Effectiveness of use of nano-structure minerals “Bentonite of Taganskiy Deposit for waste water clearing in metallurgy industry // *European Journal of Sustainable Development*. – 2014. – Vol. 3. – P.195-195. <https://doi.org/10.14207/ejsd.2014.v3n3p195>
18. Federacii G. F. R. State Pharmacopoeia of the Russian Federation. Part 1. – 2010.
19. Chernyakova R., Zh J.U., Sh S.G., Kaiynbayeva R., Kozhabekova N. Sorption of manganese (II) and vanadium (IV) cations by Tagan bentonite in an aqueous medium // *Izvestiya NAN RK. Series of Chemistry and Technology*. – 2021. – Vol. 3. – P. 68–74. <https://doi.org/10.32014/2021.2518-1491.69>
20. Rozhkova O.V., Muzdybaeva Sh.A., Bukeeva A.B., Kudajbergenova S.Zh., Rozhkov V.I., Ermekov M.T., Nurtaj Zh.T. Efficiency of using bentonite clay for treatment of mine water in the mining industry // *Vestnik KazUTB*. – 2024. – Vol. 2. – P. 460.
21. Sapargaliyev Y.M., S.A., Samatov I.B. Structural characteristics of the medicinal preparations Tagansorbent // *Geology of Kazakhstan*. – 1997. – Vol. 5. – P. 87–97.
22. Liu R., Mei X., Zhang J., Zhao D.-b. Characteristics of clay minerals in sediments of Hemudu area, Zhejiang, China in Holocene and their environmental significance // *China Geology*. – 2019. – Vol. 2. – P. 8–15. <https://doi.org/10.31035/cg2018069>
23. Daumova G.K., Abdulina S.A., Kokayeva G.A., Adilkanova M.A. Experimental studies on wastewater sorption treatment with subsequent disposal of used sorbents // *Chemical Engineering Transactions*. – 2018. – Vol. 70. – P. 2125–2130. <https://doi.org/10.3303/CET1870355>
24. Belousov P.E., Belousov P.B., Zakusin S.V., Krupskaya V.V. Quantitative methods for determining montmorillonite content in bentonite clays // *Georesursy*. – 2020. – Vol. 22. – P. 38–47. <https://doi.org/10.18599/grs.2020.3.38-47>
25. Kumari N., Mohan C. Basics of clay minerals and their characteristic properties // *Clay and Clay Minerals*. – 2021. – Vol. 24. – P.1–29. <https://doi.org/0.5772/intechopen.97672>
26. Rautureau M., Figueiredo Gomes C., Liewig N., Katouzian-Safadi M. Clays and health: Properties and therapeutic uses. *Springer Nature*. – 2017, 217p. <https://doi.org/10.1007/978-3-319-42884-0>
27. Nadziakiewicz M., Kehoe S., Micek P. Physico-chemical properties of clay minerals and their use as a health promoting feed additive // *Animals*. – 2019. – Vol. 9. – Is. 10. – P.714. <https://doi.org/10.3390/ani9100714>
28. Devapriya A., Thyagaraj T. Evaluation of red soil–bentonite mixtures for compacted clay liners // *Journal of Rock Mechanics and Geotechnical Engineering*. – 2024. – Vol. 16. – P. 697–710. <https://doi.org/10.1016/j.jrmge.2023.04.006>
29. Maged A., Kharbush S., Ismael I.S., Bhatnagar A. Characterization of activated bentonite clay mineral and the mechanisms underlying its sorption for ciprofloxacin from aqueous solution // *Environmental Science and Pollution Research*. – 2020. – Vol. 27. – P. 32980–32997. <https://doi.org/10.1007/s11356-020-09267-1>
30. Martsouka F., Papagiannopoulos K., Hatziantoniou S., Barlog M., Lagiopoulos G., Tatoulis T., Tekerlekopoulou A.G., Lampropoulou P., Papoulis D. The antimicrobial properties of modified pharmaceutical bentonite with zinc and copper // *Pharmaceutics*. – 2021. – Vol. 13. – Art.1190. <https://doi.org/10.3390/pharmaceutics13081190>
31. Kabdrakhmanova S., Joshy K., Sathian A., Aryp K., Akatan K., Shaimardan E., Beisebekov M., Gulden T., Kabdrakhmanova A., Maussumbayeva A. Anti-bacterial activity of Kalzhat clay functionalized with Ag and Cu nanoparticles // *Engineered Science*. – 2023. – Vol. 26. – Art. 972. <https://dx.doi.org/10.30919/es972>
32. Widi R., Trisulo D., Budhyantoro A., Chrisnasari R. Preparation of immobilized glucose oxidase wafer enzyme on calcium-bentonite modified by surfactant // *IOP Conference Series: Materials Science and Engineering*. – 2017. – Vol. 223. – Article 012050. <https://doi.org/10.1088/1757-899X/223/1/012050>
33. Selvasudha N., Dhanalekshmi U.-M., Krishnaraj S., et al. Multifunctional clay in pharmaceuticals // *Clay Science and Technology*. IntechOpen. – 2021. Available at: <http://dx.doi.org/10.5772/intechopen.92408>
34. Srasra E., Bekri-Abbes I. Bentonite clays for therapeutic purposes and biomaterial design // *Current Pharmaceutical Design*. – 2020. – Vol. 26, -No. 6. – P. 642–649. <https://doi.org/10.2174/1381612826666200203144034>
35. Akichoh H., Berraaouan D., Salhi S., Abdesselam T., El Miz M. Chemical and physical characterization of Moroccan bentonite taken from Nador (North of Morocco) // *American Journal of Chemistry*. – 2017. – Vol. 7, No. 4. – P. 105–112. <https://doi.org/10.5923/j.chemistry.20170704.01>

36. Elgamouz A., Tijani N., Shehadi I., Hasan K., Qawam M. Characterization of the firing behaviour of an illite-kaolinite clay mineral and its potential use as membrane support // *Heliyon*. – 2019. – Vol. 5. – Article e02281. <https://doi.org/10.1016/j.heliyon.2019.e02281>
37. Moosavi M. Bentonite clay as a natural remedy: A brief review // *Iranian Journal of Public Health*. – 2017. – Vol. 46, No. 9. – P. 1176–1183.
38. De Segonzac G.D. The transformation of clay minerals during diagenesis and low-grade metamorphism: a review // *Sedimentology*. – 1970. – Vol. 15. – P. 281–346.
39. Theng B. Negatively charged polymers (polyanions) // *Developments in Clay Science*. – 2012. – Vol. 4. – P. 111–127.
40. Kabdrakhmanova S., Aryp K., Shaimardan E., Kanat E., Selenova B., Nurgamit K., Kerimkulova A., Amitova A., Maussumbayeva A. Acid modification of clays from the Kalzhat, Orta Tentek deposits and study of their physical-chemical properties // *Materials Today: Proceedings*. – 2023. <https://doi.org/10.1016/j.matpr.2023.04.427>.
41. Ravindra R.T., Kaneko S., Endo T., Lakshmi R.S. Spectroscopic characterization of bentonite // *Journal of Lasers, Optics & Photonics*. – 2017. – Vol. 4.
42. Hayati-Ashtiani M. Characterization of nano-porous bentonite (montmorillonite) particles using FTIR and BET-BJH analyses // *Particle & Particle Systems Characterization*. – 2011. – Vol. 28. – P. 71–76.
43. Widjaya R., Juwono A., Rinaldi N. Bentonite modification with pillarization method using metal stannum // *AIP Conference Proceedings*. – 2017. – Vol. 1904. – Article 020010. <https://doi.org/10.1063/1.5011867>
44. Mekhamer W. Stability changes of Saudi bentonite suspension due to mechanical grinding // *Journal of Saudi Chemical Society*. – 2011. – Vol. 15. – P. 361–366.
45. González J.A., Ruiz M. del C. Bleaching of kaolins and clays by chlorination of iron and titanium // *Applied Clay Science*. – 2006. – Vol. 33, Iss. 3–4. – P. 219–229. <https://doi.org/10.1016/j.clay.2006.05.001>
46. Shafiq M., Alazba A.A., Amin M.T. Functionalized bentonite clay composite with NiAl-layered double hydroxide for the effective removal of Cd(II) from contaminated water // *Sustainability*. – 2022. – Vol. 14, No. 22. – P. 15462. <https://doi.org/10.3390/su142215462>
47. Tabak A., Yilmaz N., Eren E., Caglar B., Afsin B., Sarihan A. Structural analysis of naproxen-intercalated bentonite (Unye) // *Chemical Engineering Journal*. – 2011. – Vol. 174. – P. 281–288. <https://doi.org/10.1016/j.cej.2011.09.027>
48. Banik N., Jahan S., Mostofa S., Kabir H., Sharmin N., Rahman M., Ahmed S. Synthesis and characterization of organoclay modified with cetylpyridinium chloride // *Bangladesh Journal of Scientific and Industrial Research*. – 2015. – Vol. 50. – Iss. 1. – P. 65–70. <https://doi.org/10.3329/bjsir.v50i1.23812>
49. Ouhaddouch H., Cheikh A., Idrissi M.O.B., Draoui M., Bouatia M. FT-IR Spectroscopy applied for identification of a mineral drug substance in drug products: Application to bentonite // *Journal of Spectroscopy*. – 2019. – Vol. 2019. – Art. 2960845. <https://doi.org/10.1155/2019/2960845>
50. Viseras C., Carazo E., Borrego-Sánchez A., García-Villén F., Sánchez-Espejo R., Cerezo P., Aguzzi C. Clay minerals in skin drug delivery // *Clays and Clay Minerals*. – 2019. – Vol. 67. – P. 59–71. <https://doi.org/10.1007/s42860-018-0003-7>
51. Rostami-Vartooni A., Alizadeh M., Bagherzadeh M. Green synthesis, characterization and catalytic activity of natural bentonite-supported copper nanoparticles for the solvent-free synthesis of 1-substituted 1H-1,2,3,4-tetrazoles and reduction of 4-nitrophenol // *Beilstein Journal of Nanotechnology*. – 2015. – Vol. 6. – P. 2300–2309. <https://doi.org/10.3762/bjnano.6.236>

Information about authors:

Bolatkan Dana Kairatkyzy is a 2nd year PhD student at the S. Amanzholov East Kazakhstan University, (Oskemen, Kazakhstan), email: chilibayeva@mail.ru

Kerimkulova Aigul Zhadraevna, PhD is an Associate professor at Satbayev University (Almaty, Kazakhstan), e-mail: kerimkulova07@mail.ru

Beisebekov Madiyar, PhD is a Researcher at the Scientific Center of Composite Materials (Almaty, Kazakhstan), e-mail: make1987@mail.ru

Akatan Kydyrmolla, PhD is a Head of the National Scientific Laboratory for Collective Use, S.Amanzholov East Kazakhstan University (Almaty, Kazakhstan) e-mail: ahnur.hj@mail.ru

Kantai Nurgamit, PhD is a Researcher at the National Scientific Laboratory for Collective Use, S.Amanzholov East Kazakhstan University (Oskemen, Kazakhstan) e-mail: nurgan85@mail.ru

Shaimardan Yesbol, PhD is a Senior researcher at Scientific Center of Composite Materials (Almaty, Kazakhstan) e-mail: esbol_shay@mail.ru

Kukhareva Anastassiya Dmitrievna is a 2nd year master student at Satpaev university (Almaty, Kazakhstan) e-mail: kad1311@mail.ru

Bukunova Al'mira, candidate of chemical sciences is an Associate professor at School of Earth Sciences, D. Serikbayev East Kazakhstan technical university (Oskemen, Kazakhstan) e-mail: ABukunova@edu.ektu.kz

Kabdrakhmanova Sana Kanatbekovna, candidate of technical sciences is an Associate professor at the Department of Chemical and Biochemical Engineering, Satbayev University (Almaty, Kazakhstan) e-mail: sanaly33@mail.ru